Discovery and Biological Evaluation of a New Family of Potent Modulators of Multidrug Resistance: Reversal of Multidrug Resistance of Mouse Lymphoma Cells by New Natural Jatrophane Diterpenoids Isolated from *Euphorbia* Species

Judit Hohmann,*,[†] Joseph Molnár,[‡] Dóra Rédei,[†] Ferenc Evanics,[§] Peter Forgo,[∥] Alajos Kálmán,[⊥] Gyula Argay,[⊥] and Pál Szabó[⊥]

Departments of Pharmacognosy, Medical Microbiology, Pharmaceutical Analysis, and Organic Chemistry, University of Szeged, H-6720 Szeged, Hungary, and Institute of Chemistry, Chemical Research Centre, Hungarian Academy of Sciences, H-1525 Budapest, Hungary

The effects of 15 jatrophane diterpene polyesters (**1**−**3** and **5**−**16**) isolated from lipophilic extracts of *Euphorbia serrulata*, *E. esula*, *E. salicifolia*, and *E. peplus* (Euphorbiaceae) on the reversion of multidrug resistance of mouse lymphoma cells were examined. The structures of five new compounds (**1**−**5**) were elucidated by spectroscopic methods, including HRFABMS, ESIMS, ^{1}H−^{1}H homonuclear and ^{1}H−^{13}C heteronuclear correlations, long-range correlation spectra, and NOESY experiments. The stereochemistry and absolute configuration of one compound (**3**) were determined by X-ray crystallography. The structure−activity relationship is discussed.

Introduction

Resistance to multiple anticancer drugs is one of the main reasons for treatment failure in the chemotherapy of malignant tumors. A primary mechanism of multidrug resistance (MDR) is the overproduction of permeability glycoprotein (Pgp) in the plasma membranes of resistant cells, where the Pgp acts as an energy-dependent efflux pump, reducing the intracellular accumulation of anticancer drugs. Resistance mediated by Pgp is of special importance because the exposure of cancer cells to one cytostatic agent results in a specific resistance not only to the inducer but also to many other chemically unrelated anticancer drugs, representing a nonspecific cross-resistance.[1]

Pgp is a glycosylated transmembrane protein of 1280 amino acids that utilizes ATP hydrolysis energy and is encoded by the human MDR1 gene. Human Pgp is present not only in tumor cells but also in normal tissues, e.g., in the kidney, liver, small and large intestines, brain, testis, adrenal gland, and the pregnant uterus. This tissue distribution suggests that Pgp plays a significant role in the excretion of xenobiotics and metabolites into the urine and bile and into the intestinal lumen and in the prevention of their accumulation in the brain. Pgp transports structurally, chemically, and pharmacologically widely different compounds out of the cells; its substrates include various anticancer agents and also many other categories of drugs, including cardiac glycosides, immunosuppressive agents, glucocorticoids, etc.[2]

In the past few decades, extensive studies have been performed with the aim of developing effective resistance modulators or chemosensitizers to overcome the intrinsic or acquired MDR of human cancers. Potent Pgp inhibitors are being investigated in clinical trials, including calcium channel blockers such as verapamil and immunosuppressants such as cyclosporin A.[3] However, clinical application has not been attained to date because of the toxicity, undesirable side effects, and/or the low efficacy of resistance modifiers in the host organism.

In a search for MDR-reversing compounds from natural sources, *Euphorbia* (spurges) species native to Hungary were investigated. The MDR-reversing effects of lipophilic extracts of *Euphorbia esula* L., *E. peplus* L., *E. salicifolia* Host., and *E. serrulata* Thuill. were tested on mouse lymphoma cells. From the active extracts, a series of structurally related compounds were isolated and identified, revealing noteworthy Pgp inhibitory activity in the same test.

This paper reports the MDR-reversing effects produced by the extracts of *Euphorbia* species and by 15 diterpenes isolated from these extracts. We describe here the determination of the structures of five new diterpene polyesters (**1**−**5**) by means of spectroscopic investigations, including high-resolution fast-atom bombardment mass spectrometry (HRFABMS), advanced 1D and 2D NMR spectroscopy, and X-ray analysis. The structure−activity relationship is also discussed.

Results and Discussion

Methanolic extracts were prepared from fresh whole plants of *Euphorbia esula*, *E. peplus*, *E. salicifolia*, and *E. serrulata*. The methanolic extracts were concentrated and subjected to solvent partitioning to furnish dichloromethane-soluble and water-soluble fractions. The dichloromethane fractions were examined for MDR-reversing activity on mouse lymphoma cells infected with pHa MDR1/A retrovirus. All the tested extracts displayed marked effects in inhibiting the efflux pump

* To whom correspondence should be addressed. Phone: 3662545558. Fax: 3662545704. E-mail, hohmann@pharma.szote.u-szeged.hu.
   [†] Department of Pharmacognosy.
   [‡] Department of Medical Microbiology.
   [§] Department of Pharmaceutical Analysis.
   [∥] Department of Organic Chemistry.
   [⊥] Hungarian Academy of Sciences.

Table 1. Reversal of the Multidrug Resistance of Mouse Lymphoma Cells by Dichloromethane Extracts[a] of *Euphorbia* Species

species	yield of extract (g) per 100 g of fresh plant	concentration, μg/mL	FSC	SSC	FL-1	fluorescence activity ratio
E. esula	1.41	200	590.67	251.29	541.83	38.84
		2000	599.25	257.54	692.75	49.66
E. peplus	1.60	200	513.41	153.49	1627.54	79.08
		2000	461.78	169.54	491.14	23.86
E. salicifolia	1.70	200	511.84	146.17	757.66	36.81
		2000	460.70	144.77	347.77	16.89
E. serrulata	1.18	200	518.51	151.17	1778.91	86.44
		2000	460.01	157.07	428.85	20.84
verapamil		5	569.63	177.48	170.30	8.27
PAR control			559.76	190.95	1032.27	
MDR control			600.70	182.21	20.58	

[a] 50% DMSO solutions of the extracts were investigated.

activity of multidrug resistant mouse lymphoma cells (Table 1). The results obtained with the use of two different concentrations indicated that for *Euphorbia peplus*, *E. salicifolia*, and *E. serrulata*, the MDR-reversing activity was decreased at the higher concentration of the extracts. This observation can most probably be explained by the toxicity of the extracts expressed as a shrinkage of cells (FSC = forward scatter count) and the granulation that occurs on the cell surface and inside the cells (SSC = side scatter count).

The dichloromethane extracts were further studied, and various chromatographic methods, including column chromatography, flash chromatography, prepara-
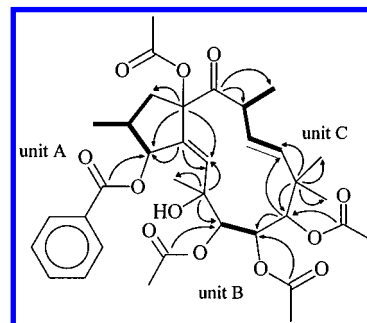
Figure 1. Selected ^{1}H–^{1}H COSY (–) and HMBC(→) correlations for **1**.

tive TLC, and HPLC, were used to isolate compounds **1**–**6** from *E. serrulata*, **7**–**10** from *E. esula*, **7** and **11** from *E. salicifolia*, and **12**–**16** from *E. peplus*.[4–8]

Compound **1** was obtained as colorless crystals. Its molecular weight was determined by HRFABMS, which indicated the molecular formula to be $C_{35}H_{44}O_{12}$. The ^{1}H NMR and JMOD (*J*-modulated spin–echo experiment) spectra of **1** showed distinct resonances for one benzoate and four acetate groups (Table 2). In combination with the ^{1}H and ^{13}C NMR data, the molecular formula suggested that **1** is a bicyclic diterpene with one disubstituted (δ_C 141.6 and 127.2, δ_H 5.47 and 5.73 dd) and one trisubstituted (δ_C 137.9 and 141.6, δ_H 5.99 brs) carbon–carbon double bond and one keto group (δ_C 204.0), satisfying the degree of unsaturation of 11. The JMOD experiment indicated that the diterpene core of the molecule is composed of five quaternary carbons, nine methine groups, one methylene, and five methyl groups. From the ^{1}H–^{1}H correlation spectroscopy (COSY) and heteronuclear multiple-quantum coherence (HMQC) spectra of **1**, three sequences of correlated protons could be extracted: $-CH_2-CH(CH_3)-CHOR-$ (fragment A), $-CHOR-CHOR-$ (fragment B), and $-CH=CH-CH-(CH_3)-$ (fragment C) (R = acyl) (Figure 1). In addition, in the ^{1}H–^{1}H COSY spectrum, weak $^4J_{H,H}$ (W-type) couplings were detected between the protons at δ_H 5.86 and 5.99 (H-3/H-5), δ_H 5.99 and 3.01 (H-5/6-OH), δ_H 5.99 and 1.13 (H-5/H-17), and δ_H 5.67 and 0.87 (H-9/H-19), indicating their close-lying position. One proton signal (δ_H 3.01 s), which did not exhibit any correlation in the HMQC spectrum, suggested one hydroxy group in the molecule. The structural fragments A–C, the quaternary carbons, the tertiary methyls, and the two methines were connected by analysis of the long-range ^{1}H–^{13}C connectivities gleaned from an heteronuclear multiple-bond correlation (HMBC) experiment (Figure 1). The HMBC cross-peaks of C-15/H-1, C-15/H-3, C-4/H-1, and
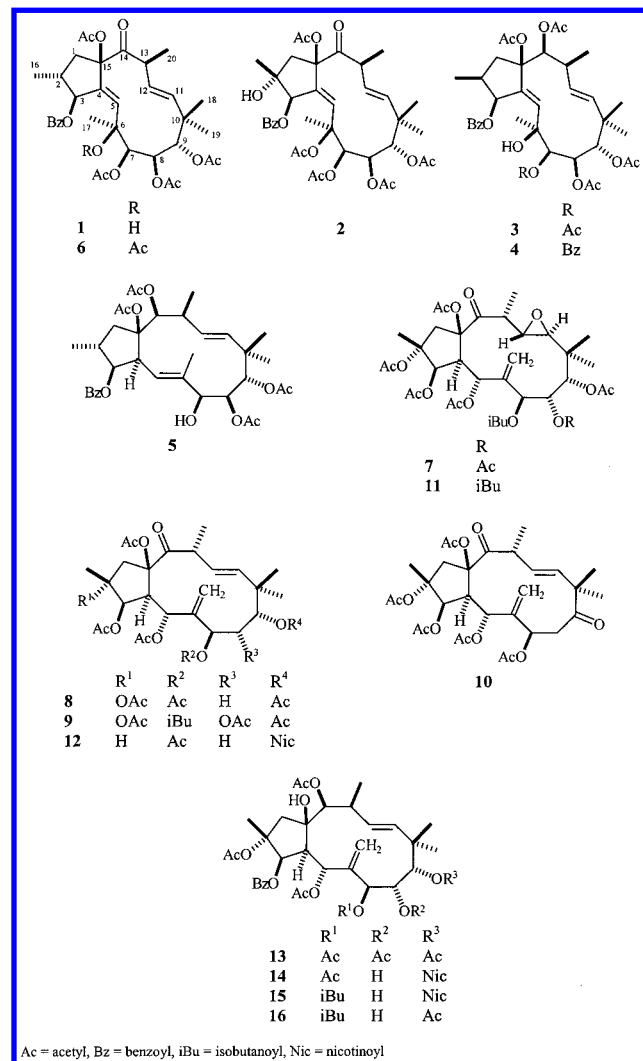

Ac = acetyl, Bz = benzoyl, iBu = isobutanoyl, Nic = nicotinoyl

Table 2. NMR Data on Compound **1** [500 MHz (^{1}H), 125 MHz (^{13}C), CDCl$_3$, δ (ppm) (J in Hz)]

atom	^{1}H	^{13}C	HMBC H no.	NOESY H no.
1β	2.71 dd (13.5, 6.6)	40.1	2, 16	1α, 2
1α	2.05 d (13.5)			1β, 3, 13, 16
2	2.33 m	40.0	1α, 16	1β, 3, 16
3	5.86 brd (5.3)	77.5	1β, 2, 5, 16	1α, 2, 7, 8, 16, 17
4		137.9	1β, 3, 5, 6-OH	
5	5.99 brs	141.6	3, 6-OH, 17	6-OH, 7, 8, 11, 17, 15Ac
6		73.7	5, 7, 17, 6-OH	
7	5.27 brs	75.8	5, 9, 6-OH, 17	3, 5, 8, 6-OH, 17, 8Ac
8	5.39 brs	67.6	7, 8Ac	5, 7, 11, 12, 19
9	5.67 s	73.7	7, 11, 18, 19	5, 6-OH, 7, 8, 11
10		41.6	8, 9, 11, 12, 18, 19	
11	5.47 d (16.3)	141.6	9, 13, 18, 19	5, 8, 9, 12, 13, 18, 19, 20
12	5.73 dd (16.3, 8.7)	127.2	13, 20	6-OH, 8, 11, 13, 18, 19, 20
13	3.70 dq (8.7, 6.9)	43.2	11, 12, 20	1α, 11, 12, 20
14		204.0	12, 13, 20	
15		90.6	1β, 3, 5	
16	1.43 d (7.0)	17.0	3, 1α, 2	1α, 2, 3
17	1.13 s	27.9	7	3, 5, 7, 2′, 6′, 6-OH
18	0.91 s	25.8	9, 11, 19	11, 12
19	0.87 s	18.0	9, 11, 18	8, 11, 12
20	1.25 d (6.9)	18.5	13	11, 12, 13
3-OBz				
CO		165.5	3, 2′, 6′	
1′		130.2	3′, 5′	
2′, 6′	8.06 d (7.8)	129.8	2′-6′	17, 15Ac
3′, 5′	7.42 t (7.8)	128.4	3′, 5′	15Ac
4′	7.54 t (7.3)	133.0	2′, 6′	
7-CO		168.9	7, 7Ac	
7-COMe	2.00 s	20.4		6-OH
8-CO		170.3	8, 8Ac	
8-COMe	2.08 s	21.0		7, 6-OH
9-CO		170.3	9, 9Ac	
9-COMe	2.12 s	21.1		
15-CO		170.9	15Ac	
15-COMe	2.12 s	21.0		5, 2′, 3′, 5′, 6′
6-OH	3.01 s			5, 7, 9, 17, 7Ac, 8Ac

C-4/H-3 suggested that partial structure A and two quaternary carbons (C-4 and C-15) were joined to a methyl-substituted five-membered ring. Similarly, the $^2J_{C-H}$ and $^3J_{C-H}$ couplings of C-4, C-6, C-9, C-10, C-14, and C-15 demonstrated that units B and C, three tertiary methyls, and two methines were connected through quaternary carbons, resulting in the 12-membered macrocycle of a jatrophane skeleton, as presented in Figure 1. The positions of the ester and hydroxy groups were also determined via the HMBC experiment. On the basis of the long-range correlations between the ester carbonyl carbons (δ_C 168.9 and 2 × 170.3) and the oxymethine protons (δ_H 5.27 brs, 5.39 brs, and 5.67 s), the presence of a benzoyl group on C-3 and of acetyl groups on C-7, C-8, and C-9 was evident. The remaining acetyl (δ_C 170.9), which did not exhibit a long-range correlation to any skeletal hydrogen, was of necessity situated on quaternary carbon C-15. The $^2J_{C-H}$ coupling between C-6 and the hydroxy group pointed to the hydroxy group being on C-6.

The relative configuration of the stereogenic centers was studied by means of a nuclear Overhauser enhancement spectroscopy (NOESY) experiment. Starting from the α position of H-3, it was found that the methyl group is in the α position at C-2 with regard to the Overhauser effect, observed for H-3/H-1α, H-1α/H-16, and H-1β/H-2. NOESY correlations between H-3 and H-17, H-3 and H-7, and H-3 and H-8 confirmed the α orientation of these protons. The β stereochemistry of H-9 and the 15-acetyl group was deduced from the interactions between 6-OH and H-9 and between the ortho benzoyl protons and the 15-OAc group. The position of H-13 followed

from the NOESY cross-peak between H-13 and H-1α. Further important NOE effects were observed between H-5 and H-11 and between H-5 and the 15-OAc group, revealing that H-5 is directed inward in the macrocyclic ring and that the C-4/C-5 olefin linkage adopts *E* stereochemistry. The above evidence led to the structure of this compound being elucidated as **1**, and complete, unambiguous ^{1}H and ^{13}C chemical shift assignments were determined as listed in Table 2. The stereochemical study of **1** indicated that the stereostructure of serrulatin B (**6**), isolated earlier from *E. serrulata*, required correction.[9] The close similarity of the ^{1}H and ^{13}C chemical shifts of **1** and **6** clearly showed that the difference in the compounds may be only the substituent on C-6. The change in the previously published β-orientation of the 16-methyl group and the α orientation of the 20-methyl group can be proposed as depicted in formula **6** with regard to the NOESY correlations between H-3 and H-1α, H-1α and H-16, and H-1α and H-13. The misinterpretation of the NOESY spectrum of **6** was due to the incorrect assignments of H-1α and H-1β.

Compound **2**, an amorphous solid, has the molecular formula C$_{37}$H$_{46}$O$_{14}$, determined via the quasimolecular ion peak at *m/z* 737.2805 [M + Na]$^+$ (calcd *m/z* 737. 2785, Δ +2.7 ppm) in the positive HRFABMS and supported by the proton and carbon counts in the NMR spectra. Comparing the ^{1}H and ^{13}C NMR spectroscopic assignments of **2** with those of **1** and taking into account their molecular formulas suggested that **2** contained an additional acetoxy group. After the ^{1}H and ^{13}C NMR signals of **2** had been assigned by interpretation of its

Table 3. NMR Data on Compounds **2**–**5** [500 MHz (^{1}H), 125 MHz (^{13}C), CDCl$_3$, δ (ppm) (J in Hz)][a]

atom	2 ^{1}H[c]	2 ^{13}C	3 ^{1}H[d]	3 ^{13}C	4[b] ^{1}H	4 ^{13}C[e]	5 1H	5 ^{13}C
1a	3.18 d (15.6)	48.0	2.45 m (2H)	43.5	2.49 m (2H)	43.1	3.59 dd (14.5, 5.7)	41.9
1b	2.16 dd (15.6, 2.0)						1.44 dd (14.5, 12.3)	
2		80.8	2.20 m	38.3	2.25 m	37.9	2.36 m	37.5
3	5.93 s	76.9	6.25 d (3.0)	77.7	6.35 d (2.9)	76.7*	4.90 t (9.1)	82.4
4		138.8		139.3			3.41 dd (9.1, 10.7)	47.3
5	6.06 s	140.0	6.63 brs	141.7	6.71 brs	141.2	5.76 d (10.7)	122.5
6		81.5		74.4		74.0		135.3
7	5.59 d (3.5)	75.3	5.85 brs	77.0	6.18 brs	76.5	3.75 brd (4.2)	78.2
8	5.34 d (3.5)	69.8	5.44 brs	69.1	5.54 brs	68.4	5.05 brd (3.1)	70.7
9	5.15 s	74.9	5.69 s	76.6	5.77 brs	76.1	4.69 brd (3.1)	74.1
10		40.8		40.4		39.8		39.8
11	5.41 d (15.9)	138.2	5.39 d (16.7)	138.1	5.42 d (16.5)	137.4	5.07 d (15.8)	135.9
12	5.58 dd (15.9, 8.7)	132.1	5.68 dd (16.7, 9.3)	134.6	5.71 dd (16.5, 9.1)	134.0	5.63 dd (15.8, 8.4)	131.8
13	4.28 dq (8.7, 6.9)	41.4	2.50 m	38.3	2.52 m	37.4	2.60 m	39.7
14		205.8	5.98 brs	78.8	6.01 brs	78.3*	4.99 d (2.7)	81.5
15		91.1		89.8		89.1		94.2
16	1.39 s	22.9	1.07 d (6.7)	22.9	1.09 d (6.2)	22.4	1.08 d (6.6)	17.5
17	1.53 s	24.7	1.11 s	29.7	1.17 s	29.2	1.69 s	16.4
18	0.92 s	25.8	0.98 s	28.4	0.99 s	27.8	1.01 s	23.8
19	0.83 s	20.3	0.90 s	22.9	0.89 s	22.0	0.91 s	21.5
20	1.22 d (6.9)	18.7	1.06 d (6.4)	14.1	1.09 d (6.2)	13.3	0.94 d (7.0)	20.8
3-OBz								
CO		165.0		165.9		165.2		167.2
1′		129.6		131.0		129.4		131.1
2′, 6′	8.01 d (7.6)	129.9	7.98 d (7.6)	130.4	8.06 d (7.3)	129.6	7.96 d (7.1)	130.2
3′, 5′	7.44 t (7.5)	128.5	7.39 t (7.6)	129.0	7.49 t (7.6)	128.3	7.39 t (7.6)	129.1
4′	7.58 t (7.4)	133.4	7.53 t (7.4)	133.6	7.60 t (7.4)	133.2	7.50 t (7.4)	133.6
6-CO		170.0†						
6-COMe	2.11 s*	20.9*						
7-CO		170.9		169.7				
7-COMe	2.19 s	21.2	2.11 s	21.3				
8-CO		172.1		171.0		170.5		170.4
8-COMe	2.10 s	22.0	2.06 s	21.8	2.09 s	20.9	2.04 s	21.7
9-CO		169.8†		171.5		170.3		172.1
9-COMe	2.10 s*	22.0*	2.21 s	21.9	2.00 s	22.0	2.10 s	21.5
14-CO				171.0		170.3		171.6
14-COMe			2.24 s	21.8	2.26 s	20.8	2.12 s	21.5
15-CO		169.1†		170.9		171.6		170.2
15-COMe	2.08 s*	20.5*	1.99 s	22.9	1.89 s	21.1	2.18 s	23.8
2-OH	3.96 d (2.0)							
6-OH			3.34 s		3.96 s			
7-OH							2.83 brd (4.2)	

[a] †Signals represented by ∗or † within the same column are interchangeable. [b] 7-OBz: δ_H 7.99 d (7.6) (H-2″, 6″), 7.39 t (7.8) (H-3″, 5″), 7.52 t (7.4) (H-4″); δ_C 165.2 (CO), 130.4 (1″), 129.6 (2″, 6″), 128.0 (3″, 5″), 132.7 (4″). [c] H-1a is in the α-position. H-1b is in the β position. [d] H-1a is in the β-position, H-1b is in the α position. [e] ^{13}C NMR signal of C-4 was not observed.

two-dimensional ^{1}H–^{1}H COSY, heteronuclear single quantum coherence (HSQC), and HMBC spectra (Table 3), it was obvious that the new oxygen function is on C-2, as a consequence of the absence of the H-2 signal and the appearance of the C-2 signal at δ_C 80.8. The positions of the ester residues on C-3, C-7, C-8, and C-9 were confirmed through the observation of long-range –C*H*–O*C*OR correlations in the HMBC spectrum. The hydroxy and acetyl groups situated on quaternary carbons (C-2, C-6, and C-15) were located by comparison of the ^{13}C chemical shifts of **2** with those of **1**, **6**,[9] and **13**–**16**,[10] proving acetoxy substitution on C-6 and C-15 [δ_{C-6} 81.8 (**6**) and 81.5 (**2**); δ_{C-15} 90.6 (**1** and **6**) and 91.1 (**2**)] and a hydroxy group on C-2, as a consequence of the upfield-shifted C-2 signal [δ_{C-2} 80.8 (**6**) and 88.3–88.5 (**13**–**16**)]. The stereochemical aspects were investigated by means of a NOESY experiment. Diagnostic NOE interactions were detected between H-3 and H-7, H-3 and H-8, H-3 and H-17, H-7 and 2-OH, H-8 and 2-OH, H-8 and H-19, and H-13 and H-1a, indicating their α stereochemistry. The Overhauser effects observed between H-1b and H-16 and between H-9 and H-18 demonstrated the β position of these protons. The

NOESY cross-peak of H-5 with H-11 pointed to the same *E* geometry of the C-4–C-5 olefin bond as found in **1**. All of the above data are compatible with structure **2** for this compound.

The structure and stereochemistry of compound **3** were determined by single-crystal X-ray analysis. The perspective view of **3** (Figure 2) depicts the absolute stereochemistry of the compound and the atomic numbering applied. A detailed NMR study of **3**, including ^{1}H–^{1}H COSY, NOESY, HSQC, and HMBC measurements, resulted in complete, unambiguous ^{1}H and ^{13}C chemical shift assignments, as listed in Table 3.

Compound **4** was isolated in a very small quantity as an amorphous solid and had a molecular weight 762 Da, as established by electrospray ionization mass spectrometry (ESIMS). Its NMR spectral data were very similar to those of **3**, differing only in the ester residue (Table 3). In the ^{1}H and ^{13}C NMR spectra of **4**, the signals for one acetate were missing, and the signals for an additional benzoyl group appeared. After the chemical shift assignment of all carbons and protons via the ^{1}H–^{1}H COSY, HSQC, and HMBC spectra, it was evident that in **4** a benzoate group is present on C-7
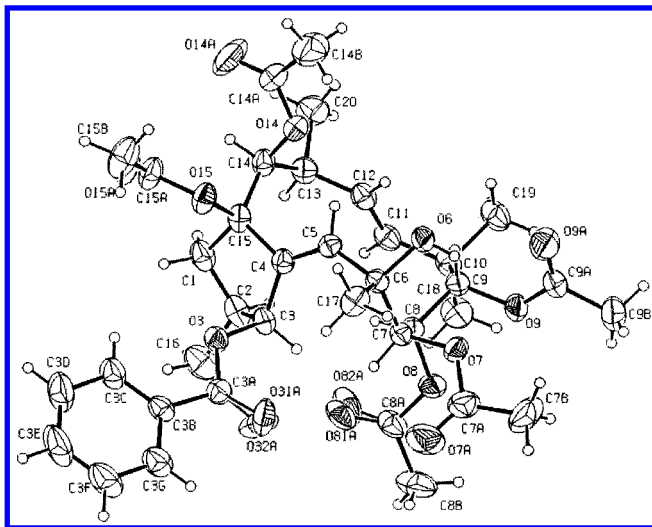
Figure 2. Perspective view of **3** using thermal ellipsoids with 30% probability level. Atomic positions of O3a and O8a are disordered with a ratio of 1:1.

because of the observed paramagnetic shifted H-7 signal [δ_{H-7} 5.85 brs (**3**) and 6.18 brs (**4**)]. The stereochemistry of **4** was investigated by NOESY measurements, with comparison of the results with those on **3**. The NOE effects and coupling constants were found to be virtually identical for **3** and **4**, and their conformations in solution were in good agreement with the solid-state conformation derived from X-ray analysis for **3**.

Compound **5**, obtained as an amorphous solid with a molecular formula of $C_{35}H_{46}O_{11}$, was shown to be a polyacylated derivative of a jatrophane diene with one benzoate and four acetate groups positioned on C-3 and on C-8, C-9, C-14, and C-15, respectively, on the basis of study of its ^{1}H and ^{13}C NMR data and 2D experiments. The ^{1}H–^{1}H COSY spectrum of **5** revealed the presence of a structural fragment $-CH_2-CH(CH_3)-$ CHOR$-CH-CH=$, which was assigned as the C-1–C-5 part of the molecule by using the heteronuclear long-range correlations extracted from an HMBC spectrum. Thus, the olefin bond in this compound is at C-5–C-6, in contrast with the other compounds obtained from *E. serrulata* (**1**–**4** and **6**). Such compounds, including the anticancer-active euphornin, were earlier isolated from *E. helioscopia* and *E. maddeni*, too.[11–13] The stereochemistry of **5** was deduced from the NOESY experiment and from the coupling constant patterns. Starting from the H-4α reference point, the NOEs of the hydrogen pairs H-4/H-13, H-4/H-14, H-14/H-1b, H-1b/H-3, and H-8/H-19 were indicative of the α orientation of these protons. Overhauser effects of the hydrogen pairs H-1a/H-2, 15-Ac/H-9, 15-Ac/H-18, H-9/H-18, and H-9/7-OH required their β orientation. The *E* geometry of the C-11–C-12 olefin linkage followed from the coupling constant of $J_{11,12} = 16$ Hz, while the *E* stereochemistry of the C-5–C-6 olefin linkage was concluded from the absence of a H-5/H-17 NOESY correlation and from the NOE-enhanced signals detected in H-4/H-17 and H-5/ 15-Ac. As concerns the conformation of the C-11–C-12 olefin linkage, the NOESY cross-peaks of H-11/H-13, H-11/H-19, H-12/H-18, and H-12/H-9 were informative, indicating that H-11 is directed below and H-12 above the plane of the macrocycle. The stereochemistry elucidated on a spectroscopic basis agreed well with the

Table 4. Reversal of the Multidrug Resistance of Mouse Lymphoma Cells by Diterpenes Isolated from *Euphorbia* Species

compound	concentration, µg/mL	FSC	SSC	FL-1	fluorescence activity ratio
1	2	562.62	237.88	532.78	8.87
	20	565.55	232.70	401.98	6.70
2	2	558.57	235.31	525.32	8.75
	20	555.80	231.39	764.30	12.73
3	2	641.56	166.49	37.12	4.31
	20	658.03	175.29	41.90	4.86
5	2	653.55	165.87	180.81	20.98
	20	654.67	167.73	299.93	34.79
6	2	561.94	238.57	634.88	10.57
	20	563.73	228.49	965.20	16.08
7	2	642.14	309.72	24.83	2.03
	20	637.57	311.17	23.61	1.93
8	2	626.30	336.52	35.43	2.47
	4	638.32	339.15	57.73	4.03
9	2	589.78	246.26	166.44	5.52
	20	620.40	254.87	444.35	14.75
10	2	642.45	313.58	31.47	2.58
	20	631.19	307.84	95.54	7.83
11	2	659.40	165.11	31.98	3.71
	20	667.76	176.12	34.14	3.96
12	2	634.95	300.61	423.87	34.74
	20	640.31	297.54	906.08	74.27
13	2	577.39	239.85	505.23	16.77
	20	587.54	239.54	888.30	29.48
14	2	632.81	301.64	155.62	12.75
	20	636.35	291.38	878.14	71.98
15	2	641.79	287.01	417.90	34.25
	20	627.99	271.93	962.29	78.88
16	2	625.31	333.78	90.12	6.30
	4	638.02	335.77	32.37	2.26
verapamil	5	569.63	177.48	170.30	8.27

calculated conformation generated with ChemWindow Suite 4.0 SymApps, version 1.01, as shown in Figure 3.

The jatrophane diterpenes **1**–**3** and **5**, elucidated above, and **6**–**16**, isolated earlier from *Euphorbia serrulata*, *E. peplus*, *E. salicifolia*, and *E. esula*,[4–8] were investigated for the reversal of MDR in mouse lymphoma cells by using the rhodamine 123 exclusion test; results are summarized in Table 4. The results show that the structurally related diterpenes differ significantly in the inhibition of the efflux pump activity of Pgp in tumor cells. Compounds **12**, **14**, and **15** derived from *E. peplus* displayed strong activity (*R* = 71.98–78.88) in reversing the MDR compared with that of the positive control verapamil (*R* = 8.27), while **7**, **8**, **10**, and **11**, obtained from *E. esula* and *E. salicifolia*, revealed only weak potency. In some cases the tested compounds (**1**, **16**) have a lower effect on the drug accumulation at higher concentration than the lowest one; in this case, the increased membrane permeability can be responsible for the toxic effect that resulted in enhanced rhodamine 123 diffusion out of the treated cells due to a membrane disintegration.

As for the structure–activity relationship, it must be stated that the tested compounds do not comprise a uniform series as regards their substitution and stereochemistry. The structural variation within the set of compounds stems from the changes in the substitution on C-2, C-8, and C-14, from the nature of the ester groups on C-3, C-7, C-8, and C-9, from the number and positions of the double bonds, and from the presence or absence of an epoxy group. Moreover, the compounds differ stereochemically in the orientation of the 16- and 20-methyls and 8-*O*-acyl groups. Comparison of the
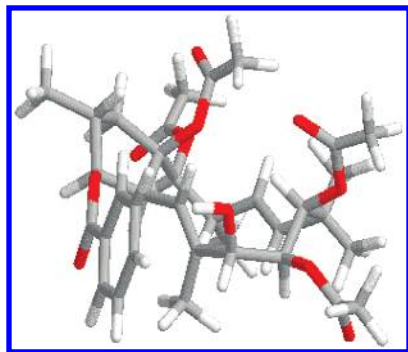
Figure 3. Calculated conformation of compound **5**.

fluorescence activity ratios, representing the anti-MDR potentials, and the structures reveals only a few relationships. Comparison of the pairs **1** and **6**, **7** and **11**, and **14** and **15**, differing only in the lipophilicity of one of the substituents (OH, OAc, OiBu), demonstrates an increase in the MDR modifier effect. These data support the conclusions that the effect on drug accumulation in drug-resistant cells is proportional to the hydrophobicity. Surprisingly, other structurally related pairs of compounds such as **8** and **12**, with 2-OAc and 2-H and with 9-OAc and 9-ONic substitutions, respectively, and **13** and **16**, differing only in the esterification at C-7–C-9 (7-OAc/7-OiBu, 8-OAc/8-OH, and 9-OAc/9-ONic), exerted very different effects in the modulation of the MDR of mouse lymphoma cells. This observation can be explained by the high flexibility of the macrocyclic ring of the jatrophane skeleton. An identical configuration at the stereogenic centers can adopt different conformations, depending mainly on the substitution pattern.[14] The conformational flexibility of the jatrophane skeleton is exemplified by the stereostructures of **3** and **5**. The X-ray molecular structure of **3** indicates a 12-membered ring in a bent arrangement, in contrast with **5**, whose macrocycle, together with the five-membered ring, is fully planar, as shown in Figure 3. The above discussion clearly reveals that a more comprehensive discussion of this SAR demands an analysis of the three-dimensional geometries.

In conclusion, this work has identified new natural products in the jatrophane diterpene group as effective lead compounds for the reversal of MDR. Quantitative three-dimensional structure–activity relationship studies and investigations aimed at a better understanding of their mechanisms of action are underway.

Experimental Section

General Experimental Procedures. Melting points are uncorrected. Mass spectroscopic measurements were carried out on a Perkin Elmer Q-STAR Pulsar Q-TOF spectrometer. NMR spectra were recorded on a Bruker Avance DRX 500 spectrometer at 500 MHz (^{1}H) and 125 MHz (^{13}C). The signals of the deuterated solvents were taken as reference. Two-dimensional experiments were performed with standard Bruker software. Optical rotations were determined in CHCl$_3$ by using a Perkin-Elmer 341 polarimeter. For column chromatography, polyamide (ICN) was used, and for flash chromatography, Si gel (Kieselgel GF$_{254}$ 15 μm, Merck) was used. Preparative TLC was performed on Si gel plates (Merck 5715). HPLC was carried out on a Waters Millipore instrument, with detection at 254 nm on LiChrospher Si 100 and on LiChrospher RP-18 (5 μm, 200 mm × 4 mm) columns with cyclohexane–EtOAc–EtOH (70:10:1) and acetonitrile–H$_2$O (4:1 and 7:3), respectively, as mobile phases.

Plant Material. *E. serrulata* was collected in June 1998 from the hill-country near Iklódbördöce, Country Zala, Hungary, and was identified by Tamás Rédei (Department of Taxonomy and Ecology, Eötvös Lóránd University, Budapest, Hungary). A voucher specimen (no. 510) has been deposited in the Herbarium of the Department of Pharmacognosy, University of Szeged, Szeged, Hungary.

Extraction and Isolation. The fresh plant material of *E. serrulata* (2400 g) was percolated with MeOH (19 L) at room temperature. The crude extract was concentrated in vacuo to 500 mL and exhaustively extracted with *n*-hexane (1800 mL). On evaporation, the organic phase gave a residue (16 g), which was chromatographed on a polyamide column (72 g) with mixtures of MeOH and H$_2$O (3:2 and 4:1) as eluents. The fractions obtained with MeOH–H$_2$O (3:2) were subjected to silica gel (60 g) flash chromatography, using a gradient system of petroleum ether–EtOAc (49:1, 9:1, 4:1, 7:3, and 1:1). Fractions 35–47, eluted with petroleum ether–EtOAc (7:3), were subjected repeatedly to silica gel flash chromatography, using benzene–CHCl$_3$–diethyl ether mixtures of increasing polarity. Fractions 3–7, obtained with the first eluent (10:5:1), were further fractionated by NP-HPLC with *n*-hexanes–EtOAc–EtOH (70:10:1) as eluent and then further purified by RP-HPLC, using acetonitrile–H$_2$O (4:1), to yield **5** (10.6 mg). Fraction 8 from the second flash chromatography was rechromatographed by RP-HPLC with acetonitrile–H$_2$O (7:3) to furnish **1** (14.4 mg), **2** (5.9 mg), and **4** (1.0 mg). Fractions 48–51, obtained from the first flash chromatography with petroleum ether–EtOAc (1:1), after NP-HPLC separation with cyclohexanes–EtOAc–EtOH (130:30:3), afforded **3** (5.2 mg).

(2R^*,3S^*,6S^*,7R^*,8R^*,9S^*,13S^*,15R^*)-7,8,9,15-Tetra-acetoxy-3-benzoyloxy-6-hydroxy-14-oxojatropha-4E,11E-diene (1): colorless crystals; mp 220–223 °C; [α]$^{25}_{\rm D}$ −98° (*c* 0.06, CHCl$_3$); UV $\lambda_{\rm max}$ (log ϵ) (MeOH) 229 (3.80), 273 (2.73), 281sh (2.67); HRESIMS *m/z* 789.1902 [M + Cs]$^+$ (calcd for 789.1887, Δ −1.9 ppm, C$_{35}$H$_{44}$O$_{12}$Cs); ^{1}H and ^{13}C NMR, see Table 2.

(2R^*,3R^*,6S^*,7R^*,8R^*,9S^*,13S^*,15R^*)-6,7,8,9,15-Penta-acetoxy-3-benzoyloxy-2-hydroxy-14-oxojatropha-4E,11E-diene (2): amorphous solid; [α]$^{25}_{\rm D}$ −18° (*c* 0.12, CHCl$_3$); UV $\lambda_{\rm max}$ (log ϵ) (MeOH) 231 (3.75), 275 (2.78), 282 sh (2.72); HRESIMS *m/z* 737.2805 [M + Na]$^+$ (calcd for *m/z* 737.2785, Δ +2.7 ppm, C$_{37}$H$_{46}$O$_{14}$); ^{1}H and ^{13}C NMR, see Table 3.

(2S,3S,6S,7R,8R,9S,13S,14S,15R)-7,8,9,14,15-Pentaace-toxy-3-benzoyloxy-6-hydroxyjatropha-4E,11E-diene (3): white needles; mp 196–199 °C; [α]$^{25}_{\rm D}$ −80° (*c* 1.5, CHCl$_3$); UV $\lambda_{\rm max}$ (log ϵ) (MeOH) 230 (3.92), 273 (2.80), 281 sh (2.72); HRFABMS *m/z* 723.3005 [M + Na]$^+$ (calcd for *m/z* 723.2993, Δ +2.2 ppm, C$_{37}$H$_{48}$O$_{13}$); ^{1}H and ^{13}C NMR, see Table 3.

(2S^*,3S^*,6S^*,7R^*,8R^*,9S^*,13S^*,14S^*,15R^*)-8,9,14,15-Tet-raacetoxy-3,7-dibenzoyloxy-6-hydroxyjatropha-4E,11E-diene (4): amorphous solid; [α]$^{25}_{\rm D}$ −15° (*c* 0.05, CHCl$_3$); UV $\lambda_{\rm max}$ (log ϵ) (MeOH) 230 (3.90), 273 (2.82), 282 sh (2.75); HRESIMS *m/z* 895.2361 [M + Cs]$^+$ (calcd for *m/z* 895.2306, Δ −1.1 ppm, C$_{42}$H$_{50}$O$_{13}$Cs); ^{1}H and ^{13}C NMR, see Table 3.

(2R^*,3S^*,4S^*,7S^*,8S^*,9S^*,13S^*,14S^*,15R^*)-8,9,14,15-Tet-raacetoxy-3-benzoyloxy-7-hydroxyjatropha-5E,11E-di-ene (5): amorphous solid; [α]$^{25}_{\rm D}$ −107° (*c* 0.2, CHCl$_3$); UV $\lambda_{\rm max}$ (log ϵ) (MeOH) 229 (3.91), 274 (2.79), 281 sh (2.69); HRESIMS *m/z* 775.2124 [M + Cs]$^+$ (calcd for *m/z* 775.2094, Δ −3.8 ppm, C$_{35}$H$_{46}$O$_{11}$Cs); ^{1}H and ^{13}C NMR, see Table 3.

Crystal Structure Determination of 3. Diffraction data were collected from a single crystal of 0.30 mm × 0.20 mm × 0.10 mm, using a CAD-4 diffractometer with graphite-mono-chromated Cu Kα radiation (λ = 1.5418 Å). C$_{37}$H$_{48}$O$_{13}$, M = 700.75, orthorhombic, space group (from systematic absences) $P2_12_12_1$, a = 10.397(1) Å, b = 17.031(1) Å, c = 22.050(2) Å, V = 3904.0(6) Å^3, D_c(Z=4) =1.192 g cm^{-3}. The structure was solved by direct methods with SHELXS-97[15] and was refined by full-matrix least-squares in F^2 mode using SHELXL-97.[16] Hydrogen positions were calculated from assumed geometries and included in SF calculations but without refinement. Reflections measured were 9028, unique reflections were 7807

$[I > 2\sigma(I)]$ 4431, $R = 0.047$, $R_w^2 = 0.118$. The absolute structure was determined by refining the Flack[17] parameter to 0.00(19). The molecular plot was drawn with the program ORTEP-III.[18] (The crystal structure has been deposited at the Cambridge Crystallographic Data Centre. Deposition number is CCDC-173593.)

Cell and Fluorescence Uptake, MDR Reversal Effect. The L5178 mouse T cell lymphoma cell line was infected with the pHa MDR1/A retrovirus as previously described.[19] MDR1 expressing cell lines were selected by culturing the infected cells with 60 ng/mL colchicine to maintain expression of the MDR phenotype. The L5178 MDR cell line and the L5178Y parent cell line were grown in McCoy's 5AA medium with 10% heat-inactivated horse serum, L-glutamine, and antibiotics. The cells were adjusted to a concentration of 2×10^6/mL, resuspended in serum-free McCoy's 5AA medium, and distributed in 0.5 mL aliquots into Eppendorf centrifuge tubes. From 2.0 to 20.0 μL aliquots of the 1.0 mg/mL stock solutions of the tested compounds in DMSO were then added, and the samples were incubated for 10 min at room temperature. A total of 10 μL (5.2 μM final concentration) of the indicator rhodamine 123 was next added to the samples, and the cells were incubated for a further 20 min at 37 °C, washed twice, and resuspended in 0.5 mL of phosphate-buffered saline for analysis. The fluorescence of the cell population was measured by flow cytometry with a Beckton Dickinson FACScan instrument. Verapamil was used as a positive control in the rhodamine 123 exclusion experiments. The fluorescence activity ratio was calculated from the drug accumulation of treated MDR and untreated MDR cells related to parental treated per untreated drug sensitive cells. An activity ratio (R) was calculated on the basis of the measured fluorescence values via the following equation:

$$R = \frac{\text{MDR treated/MDR control}}{\text{parental treated/parental control}}$$

The degree of purity of all tested compounds (**1**–**3** and **5**–**16**) was over 95%, as documented by the HPLC and ^{1}H NMR spectra.

Supporting Information Available: HPLC chromatograms for compounds **1**–**3**, **5**, **6**, and **14**–**16** and ^{1}H NMR spectra for **7**–**13** demonstrating the purity of the compounds. This material is available free of charge via the Internet at http://pubs.acs.org.

References

(1) Szabó, D.; Keyzer, H.; Kaiser, H. E.; Molnár, J. Reversal of multidrug resistance of tumour cells. *Anticancer Res.* **2000**, *20*, 4261−4274.

(2) Blackmore, C. G.; McNaughton, P. A.; van Veen, H. W. Multidrug transporters in prokaryotic and eukaryotic cells: physiological functions and transport mechanisms. *Mol. Membr. Biol.* **2001**, *18*, 97−103.

(3) Ford, J. M.; Hait, W. N. Pharmacology of drugs that alter multidrug resistance in cancer. *Pharmacol. Rev.* **1990**, *42*, 155−199.

(4) Hohmann, J.; Vasas, A.; Günther, G.; Máthé, I.; Evanics, F.; Dombi, Gy.; Jerkovich, Gy. Macrocyclic diterpene polyesters of the jatrophane type from *Euphorbia esula*. *J. Nat. Prod.* **1997**, *60*, 331−335.

(5) Günther, G.; Hohmann, J.; Vasas, A.; Máthé, I.; Dombi, Gy.; Jerkovich, Gy. Jatrophane diterpenoids from *Euphorbia esula*. *Phytochemistry* **1998**, *47*, 1309−1313.

(6) Günther, G.; Martinek, T.; Dombi, Gy.; Hohmann, J.; Vasas, A. Structural characterisation and dynamic NMR studies of a new peracylated macrocyclic diterpene. *Magn. Reson. Chem.* **1999**, *37*, 365−370.

(7) Hohmann, J.; Evanics, F.; Dombi, Gy.; Molnár, J.; Szabó, P. Euphosalicin, a new diterpene polyester with multidrug resistance reversing activity from *Euphorbia salicifolia*. *Tetrahedron* **2001**, *57*, 211−215.

(8) Hohmann, J.; Vasas, A.; Günther, G.; Dombi, Gy.; Blazsó, G.; Falkay, Gy.; Máthé, I.; Jerkovich, Gy. Jatrophane diterpenoids from *Euphorbia peplus*. *Phytochemistry* **1999**, *51*, 673−677.

(9) Hohmann, J.; Rédei, D.; Evanics, F.; Kálmán, A.; Argay, Gy.; Bartók, T. Serrulatin A and B, new diterpene polyesters from *Euphorbia serrulata*. *Tetrahedron* **2000**, *56*, 3619−3623.

(10) Jakupovic, J.; Morgenstern, T.; Bittner, M.; Silva, M. Diterpenes from *Euphorbia peplus*. *Phytochemistry* **1998**, *47*, 1601−1609.

(11) Sahai, R.; Rastogi, R. P.; Jakupovic, J.; Bohlmann, F. A diterpene from *Euphorbia maddeni*. *Phytochemistry* **1981**, *20*, 1665−1667.

(12) Yamamura, S.; Kosemura, S.; Ohba, S.; Ito, M.; Saito, Y. The isolation and structures of euphoscopins A and B. *Tetrahedron Lett.* **1981**, *22*, 5315−5318.

(13) Yamamura, S.; Shizuri, Y.; Kosemura, S.; Ohtsuka, J.; Tayama, T.; Ohba, S.; Ito, M.; Saito, Y.; Terada, Y. Diterpenes from *Euphorbia helioscopia*. *Phytochemistry* **1989**, *28*, 3421−3436.

(14) Appendino, G.; Jakupovic, S.; Tron, G. C.; Jakupovic, J.; Milon, V.; Ballero, M. Macrocyclic diterpenoids from *Euphorbia semiperfoliata*. *J. Nat. Prod.* **1998**, *61*, 749−756.

(15) Sheldrick, G. M. *SHELXS-97. Program for structure solution*; University of Göttingen: Göttingen, Germany 1997.

(16) Sheldrick, G. M. *SHELXL-97. Program for structure refinement*; University of Göttingen: Göttingen, Germany 1997.

(17) Flack, H. D. On enantiomorph-polarity estimation. *Acta Crystallogr.* **1983**, *A39*, 876−881.

(18) Burnett, M. N.; Johnson, C. K. *ORTEP-III. Oak Ridge Thermal Ellipsoid Plot Program for Crystal Structure Illustrations*; Report ORNL-6895; Oak Ridge National Laboratory: Oak Ridge, TN, 1996. Windows implementation was by Farrugia, L. J., Department of Chemistry, University of Glasgow, UK, 1998.

(19) Cornwell, M. M.; Pastan, I.; Gottesmann, M. M. Certain calcium channel blockers bind specifically to multidrug-resistant human KB carcinoma membrane vesicles and inhibit drug binding to P-glycoprotein. *J. Biol. Chem.* **1987**, *262*, 2166−2170.

JM0111301